Supporting Information

Metal-Organic Frameworks as Electrolyte Additives to Enable Ultrastable Plating/Stripping of Li Anode with Dendrite Inhibition

Fulu Chu[†,‡], Jiulin Hu[†], Chenglong Wu[†], Zhenguo Yao[†], Jing Tian[†], Zheng Li[*,‡], and Chilin Li[*,†]

[†]State Key Laboratory of High Performance Ceramics and Superfine Microstructure, Shanghai Institute of Ceramics, Chinese Academy of Sciences, 1295 Ding Xi Road, Shanghai 200050, China. Email: chilinli@mail.sic.ac.cn

[‡]School of Materials Science and Engineering, Xiangtan University, Xiangtan 411105, China. Email: lizheng@xtu.edu.cn

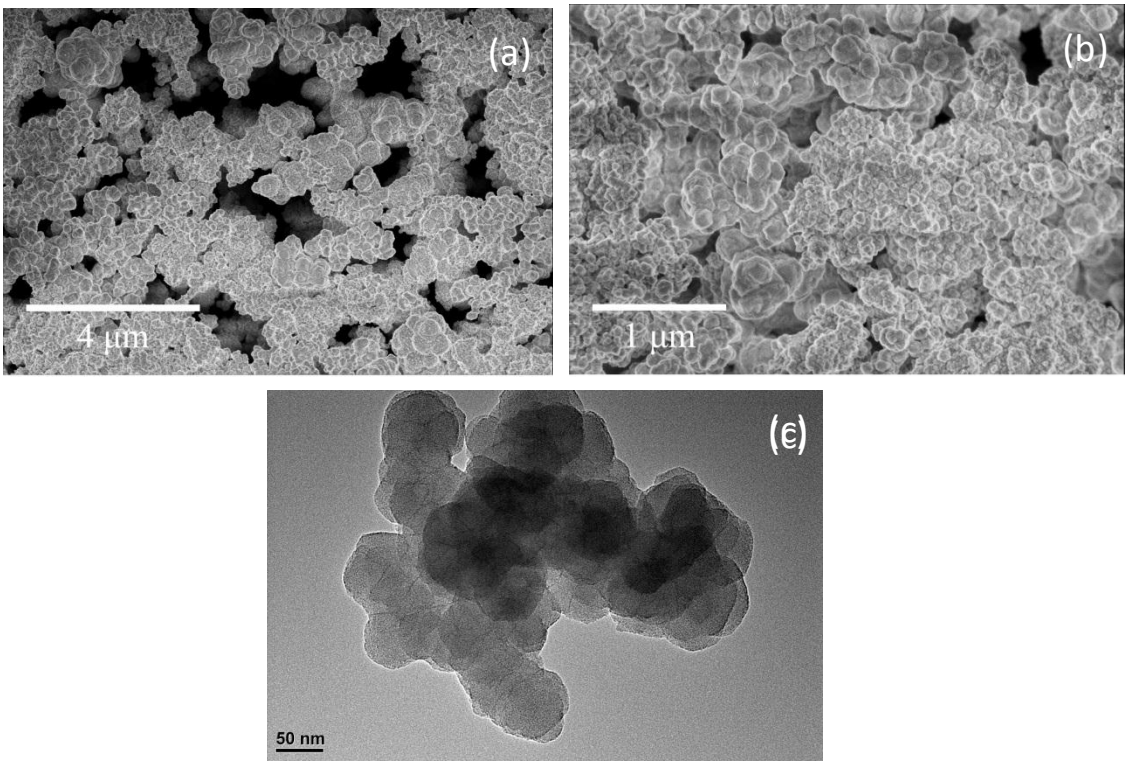

Figure S1. (a, b) SEM images of UiO-66 grains with different scale. (c)TEM image of UiO-66 grains.

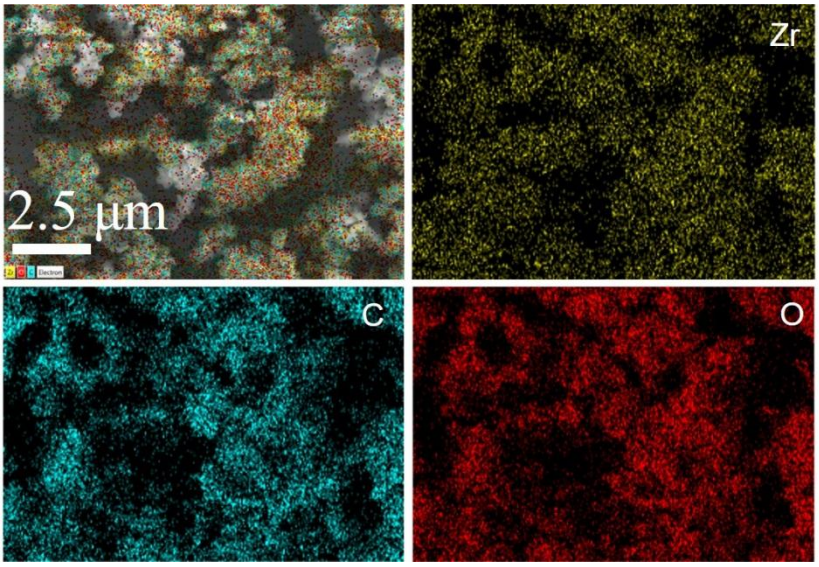

Figure S2. EDX element mapping of Zr, C and O in UiO-66.

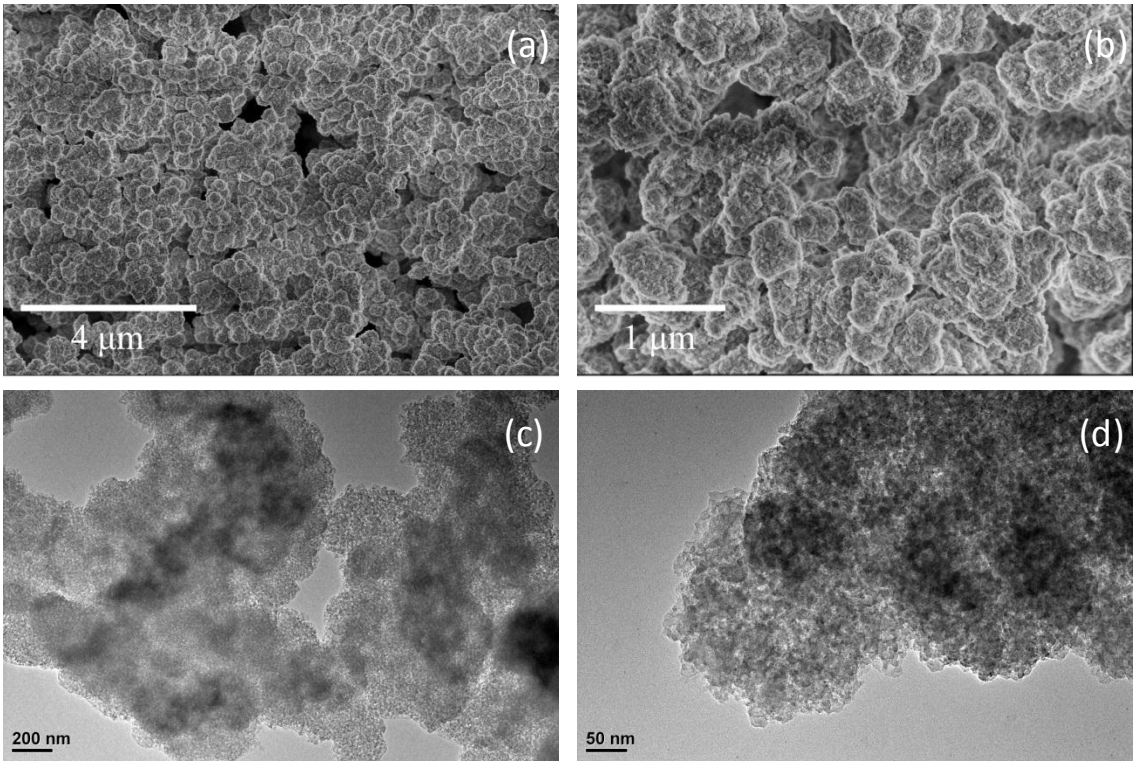

Figure S3. (a, b) SEM images of MIL-101-NH_2 grains with different scale. (c, d) TEM image of MIL-101-NH_2 grains with different scale.

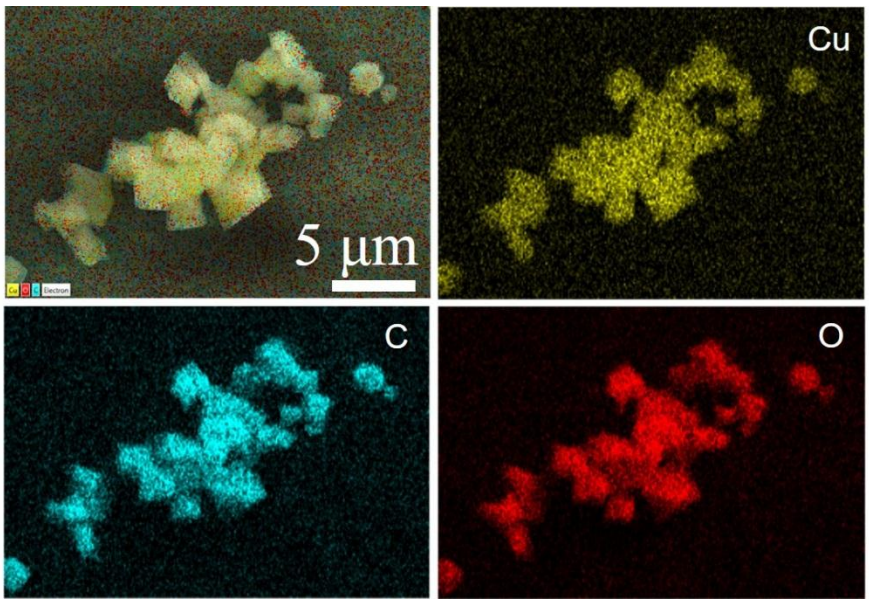

Figure S4. EDX element mapping of Cu, C and O in HKUST-1.

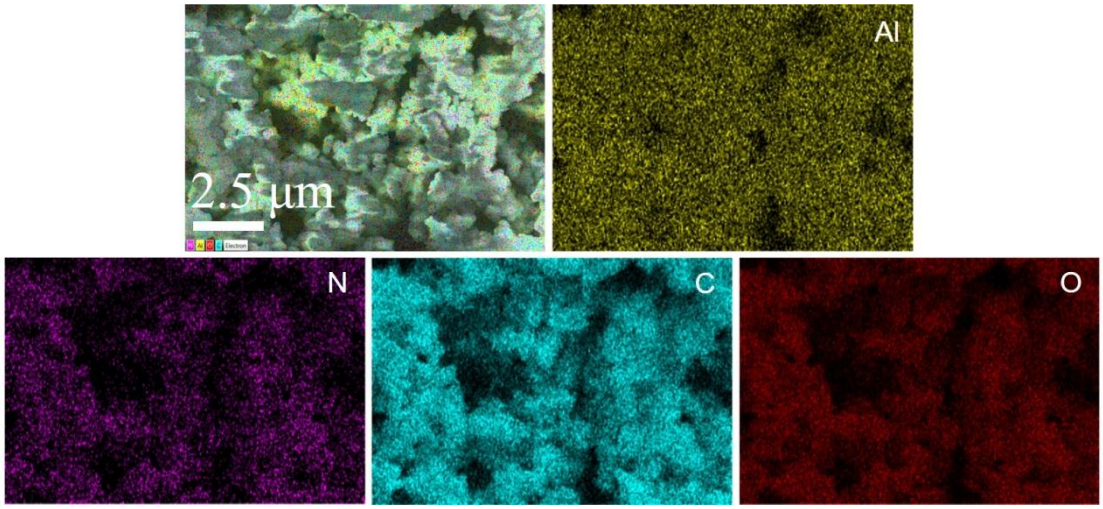

Figure S5. EDX element mapping of Al, N, C and O in MIL-101-NH_2.

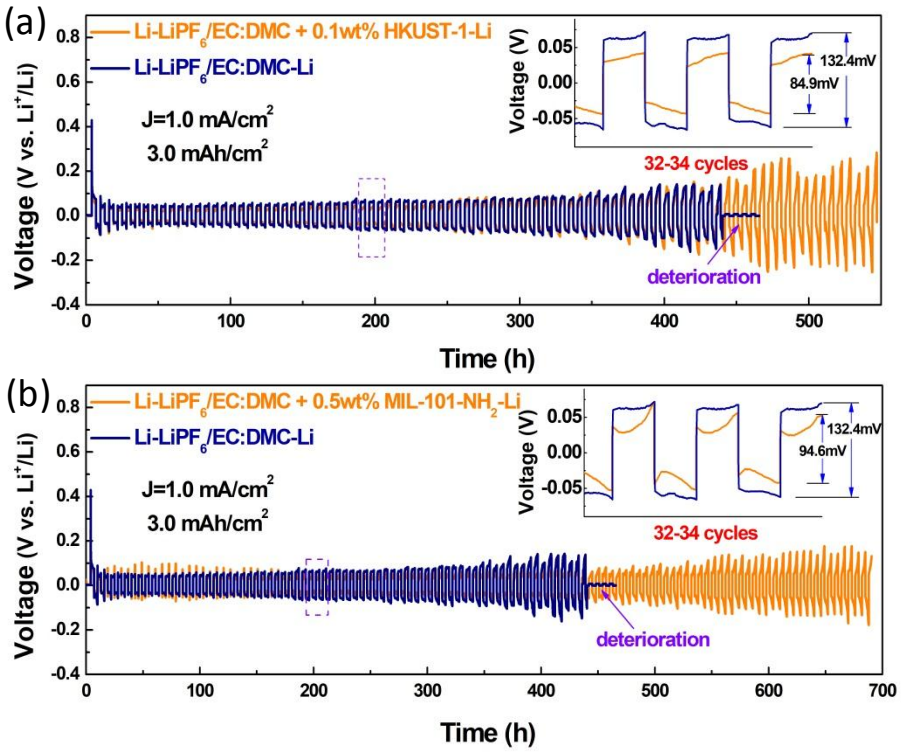

Figure S6. Li plating/stripping performance of Li||Li symmetric cells with (a) 0.1wt% HKUST-1 and (b) 0.5wt% MIL-101-NH_2 at 1 mA/cm^2 with an areal capacity of 3 mAh/cm^2. The performance of Li||Li symmetric cell free of MOF additive is also shown as a reference. Insets: corresponding voltage profiles during 32-34 cycles.

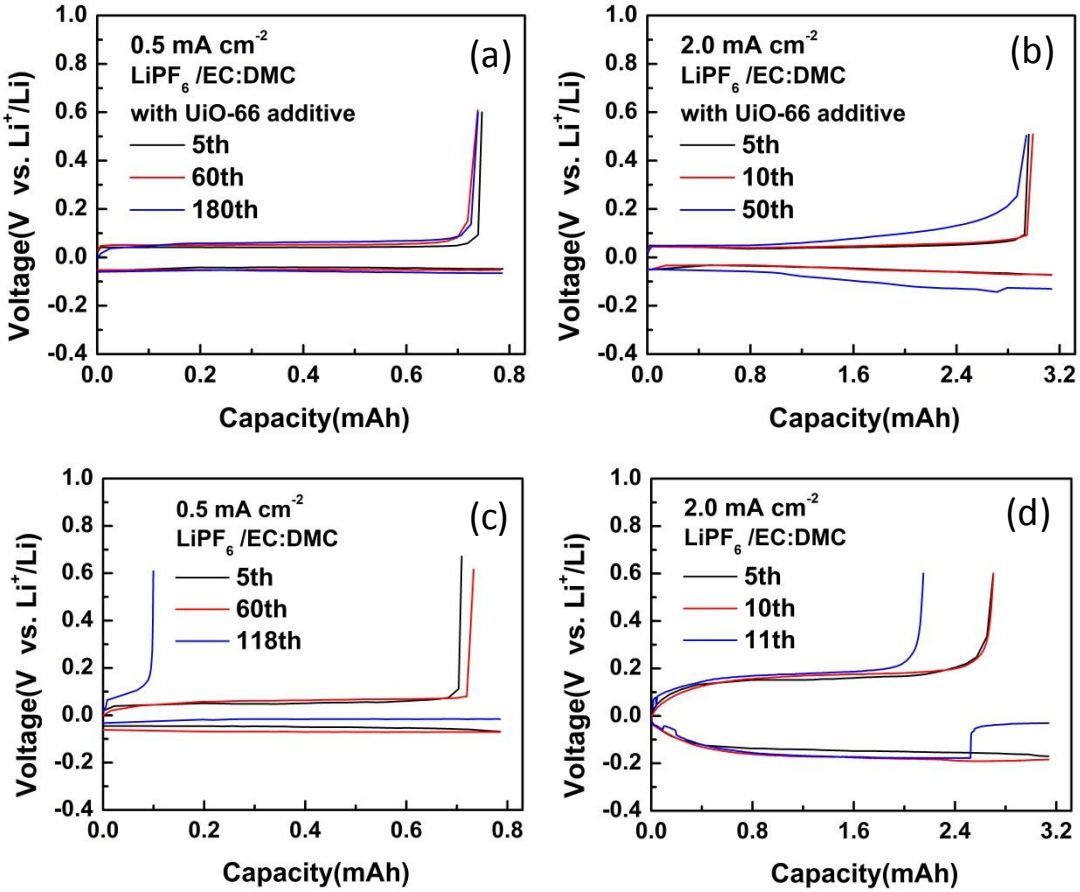

Figure S7. Voltage profiles of Li||Cu asymmetric cells with UiO-66 additive at different cycling stages at (a) 0.5 mA/cm^2 and (b) 2 mA/cm^2. Voltage profiles of Li||Cu asymmetric cells free of MOF additive at different cycling stages at (c) 0.5 mA/cm^2 and (d) 2 mA/cm^2.

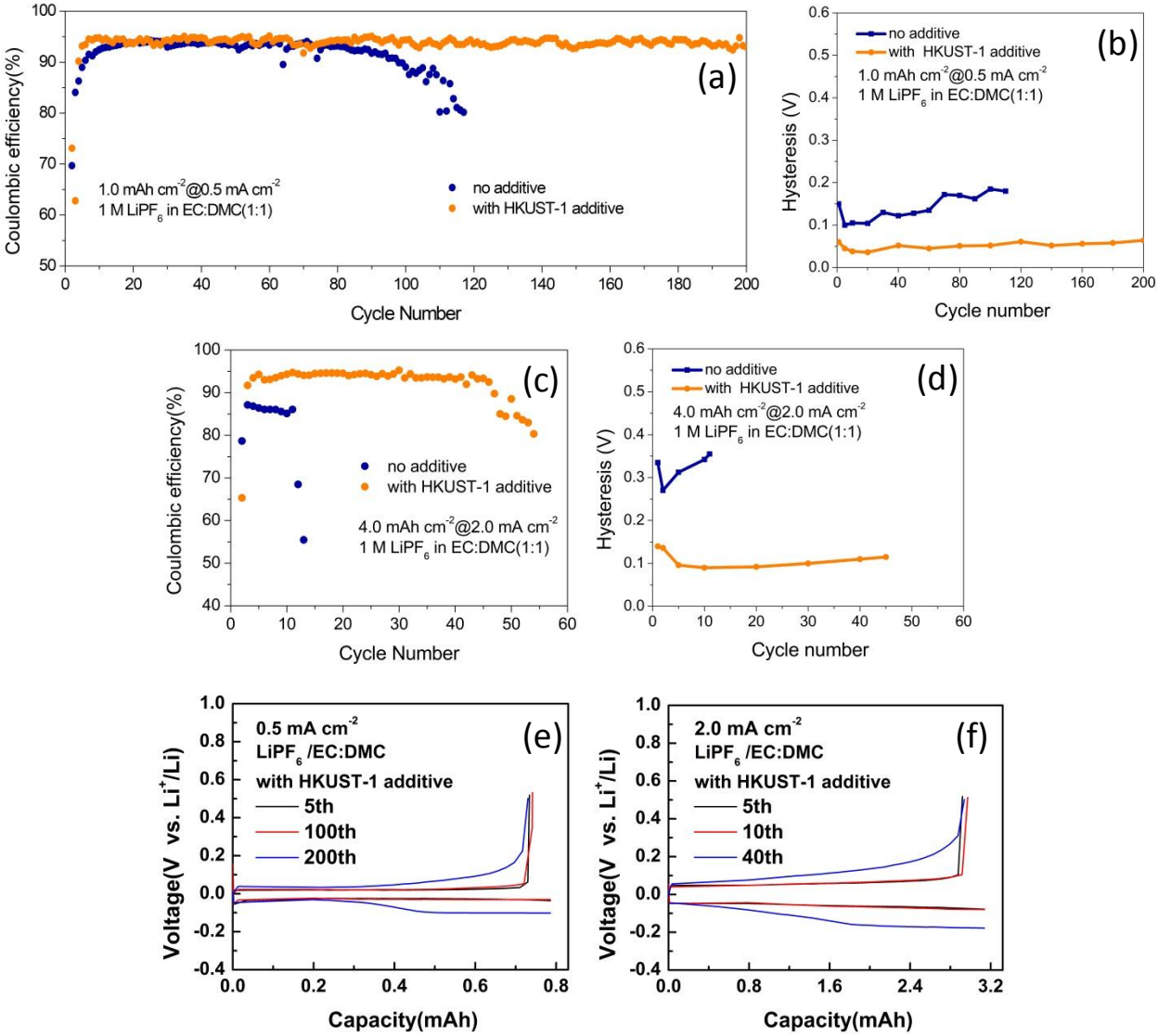

Figure S8. Comparison of Coulombic efficiency as a function of cycle number in $LiPF_6$-EC-DMC system with 0 and 1.0 wt% HKUST-1 as additive (a) at 0.5 mA/cm^2 with a capacity of 1 mAh/cm^2 and (c) at 2 mA/cm^2 with a capacity of 4 mAh/cm^2. Corresponding voltage hysteresis as a function of cycle number at (b) 0.5 and (d) 2 mA/cm^2. Voltage profiles of Li||Cu asymmetric cells with HKUST-1 additive at different

cycling stages at (e) 0.5 mA/cm^2 and (f) 2 mA/cm^2.

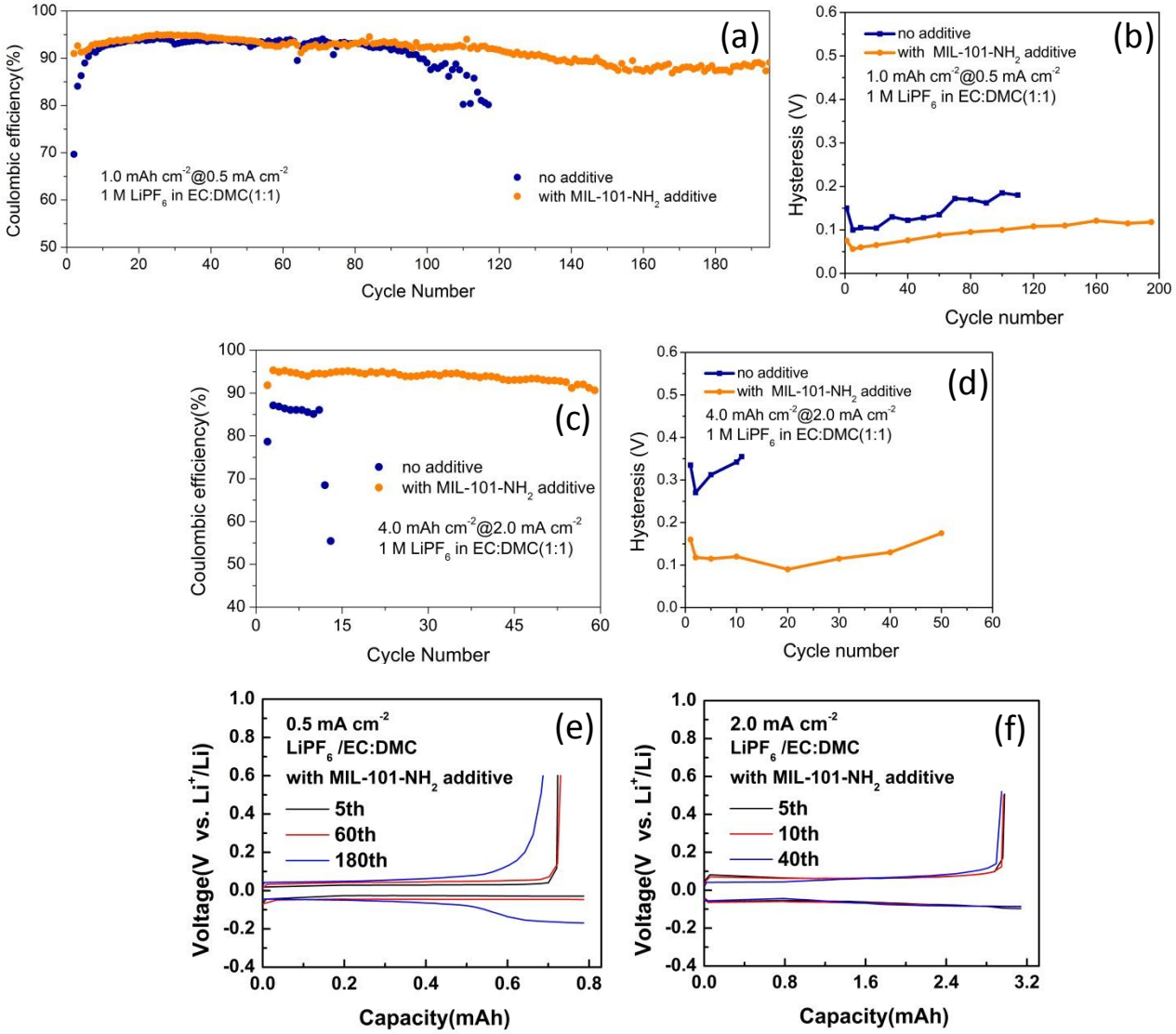

Figure S9. Comparison of Coulombic efficiency as a function of cycle number in $LiPF_6$-EC-DMC system with 0 and 1.0 wt% MIL-101-NH_2 as additive (a) at 0.5 mA/cm^2 with a capacity of 1 mAh/cm^2 and (c) at 2 mA/cm^2 with a capacity of 4 mAh/cm^2. Corresponding voltage hysteresis as a function of cycle number at (b) 0.5 and (d) 2 mA/cm^2. Voltage profiles of Li||Cu asymmetric cells with MIL-101-NH_2 additive at

different cycling stages at (e) 0.5 mA/cm^2 and (f) 2 mA/cm^2.

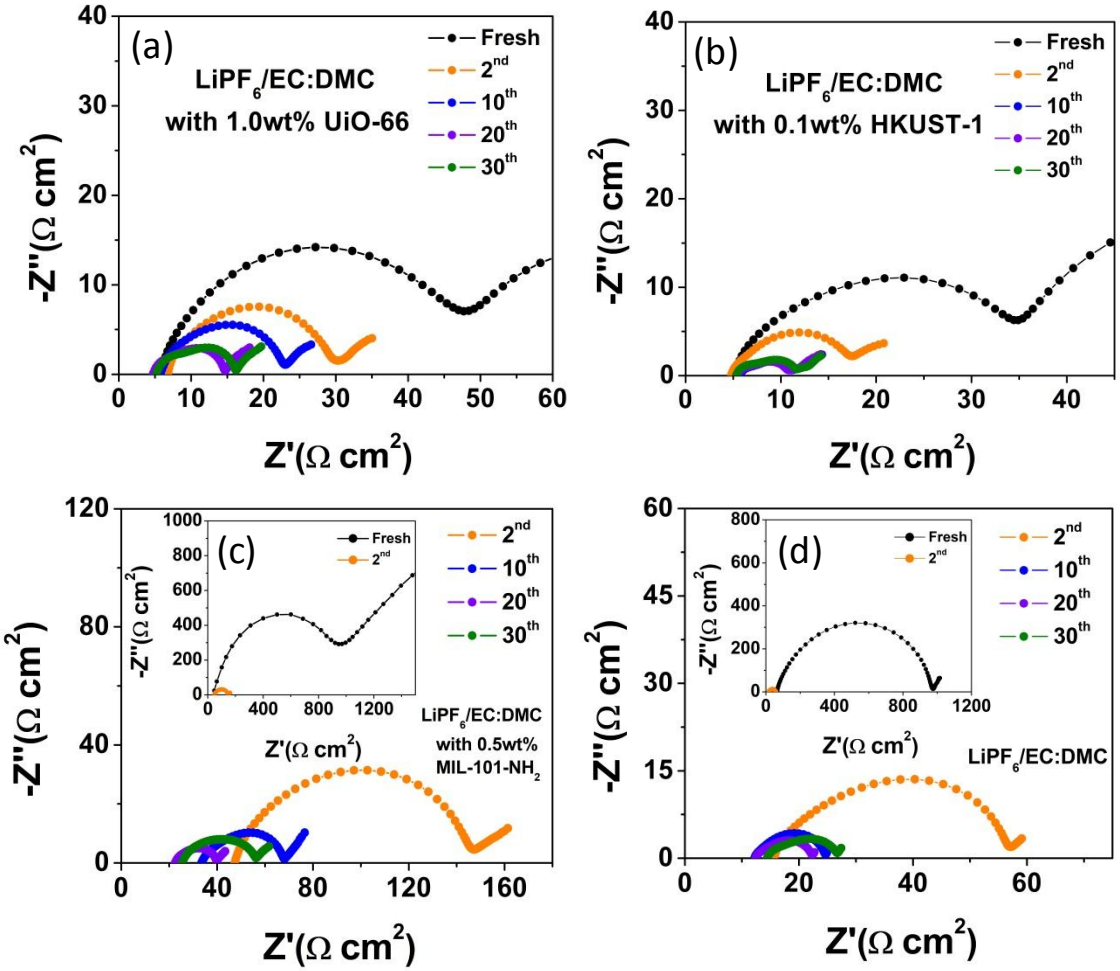

Figure S10. Electrochemical impedance spectra of Li||Li symmetric cells at different cycling stages for (a) 1 wt% UiO-66-contained, (b) 0.1 wt% HKUST-1-contained, (c) 0.5 wt% MIL-101-NH_2-contained and (d) additive-free $LiPF_6$-EC-DMC systems at 0.5 mA/cm^2 with an areal capacity of 1.5 mAh/cm^2. Insets of (c,d): electrochemical impedance spectra of Li||Li symmetric cells before cycling and after 2 cycles for the (c) MIL-101-NH_2-contained and (d) additive-free systems.

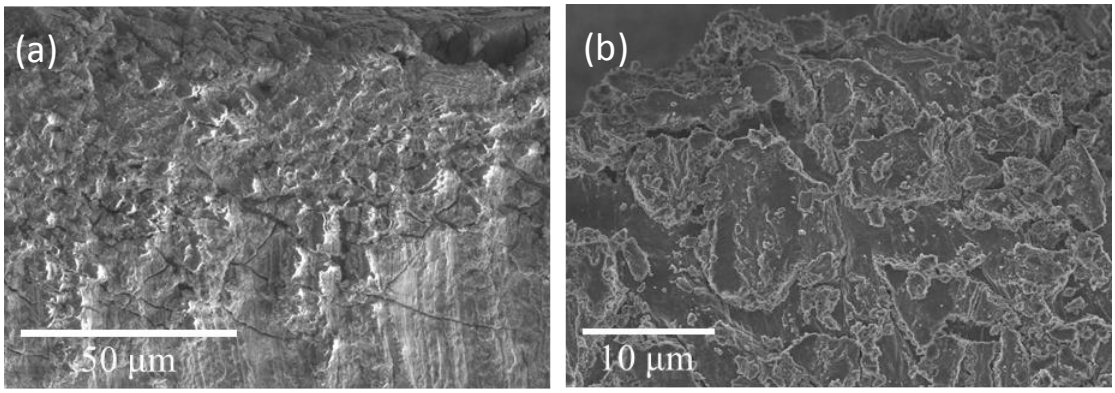

Figure S11. Cross-section SEM images of cycled Li morphology at Li plating stage based on Li||Li symmetric cells after 60 cycles for 1wt% UiO-66-contained $LiPF_6$-EC-DMC system, focusing on (a) the interface region between plated Li and unreacted Li as well as (b) the near-surface region.

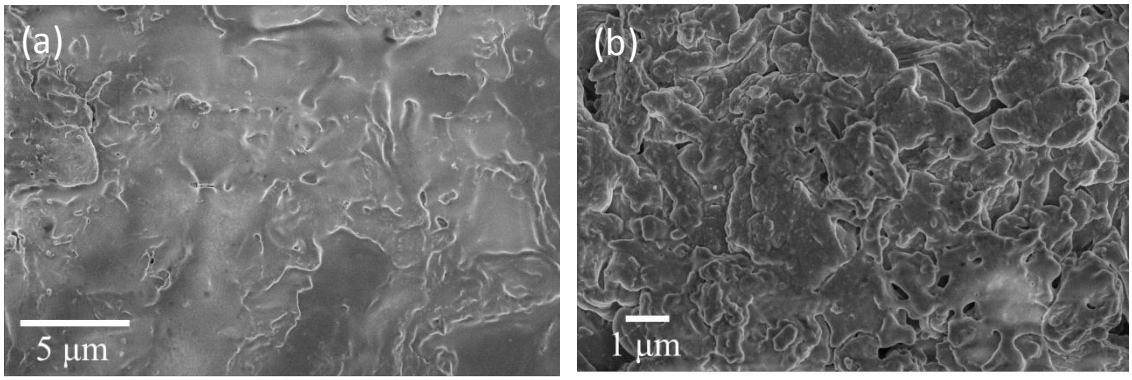

Figure S12. (a) Overview and (b) magnified SEM images of cycled Li surface morphology at Li plating stage based on Li||Li symmetric cells with 0.1wt% HKUST-1 after 60 cycles at 1 mA/cm^2 with a capacity of 3 mAh/cm^2.

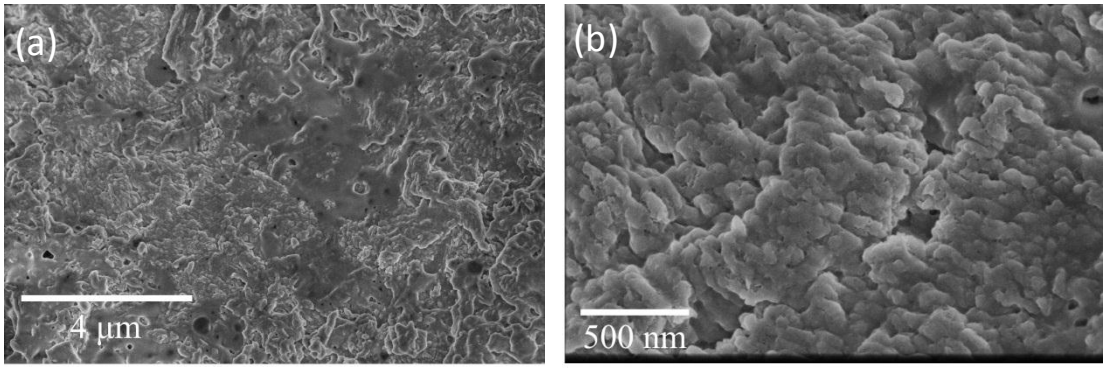

Figure S13. (a) Overview and (b) magnified SEM images of cycled Li surface morphology at Li plating stage based on Li||Li symmetric cells with 0.5wt% MIL-101-NH_2 after 60 cycles at 1 mA/cm^2 with a capacity of 3 mAh/cm^2.

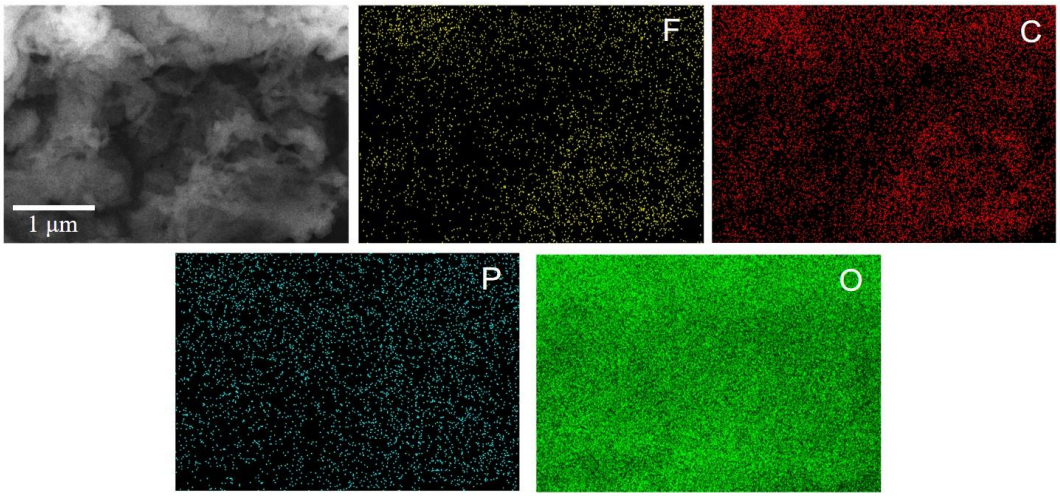

Figure S14. EDX mapping images of cycled Li anode at Li plating stage based on Li||Li symmetric cell after 60 cycles for additive-free $LiPF_6$-EC-DMC systems.

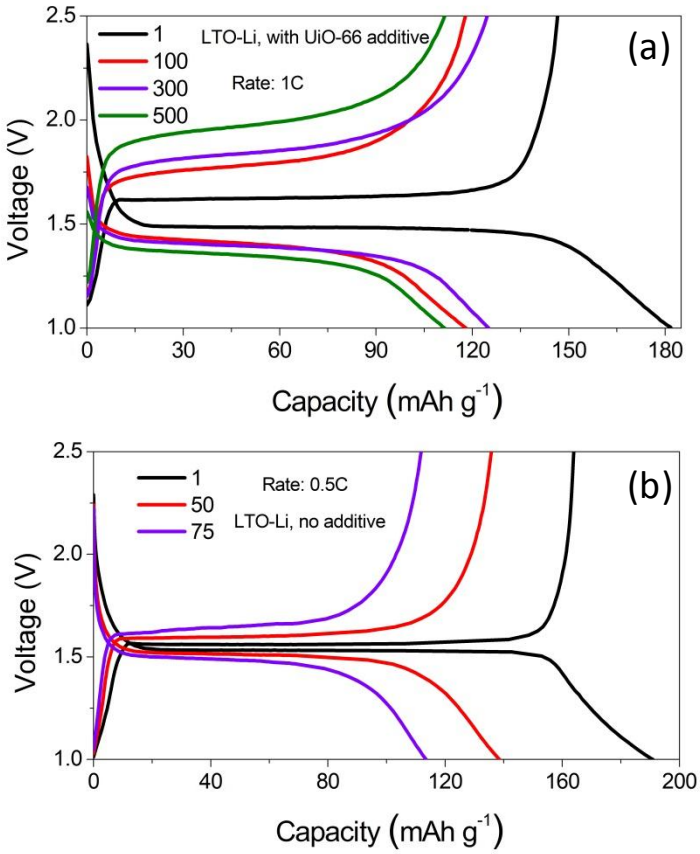

Figure S15. Voltage curves of Li/LTO cells (a) with UiO-66 as additive at 1C and (b) without additive at 0.5C at different cycling stages.

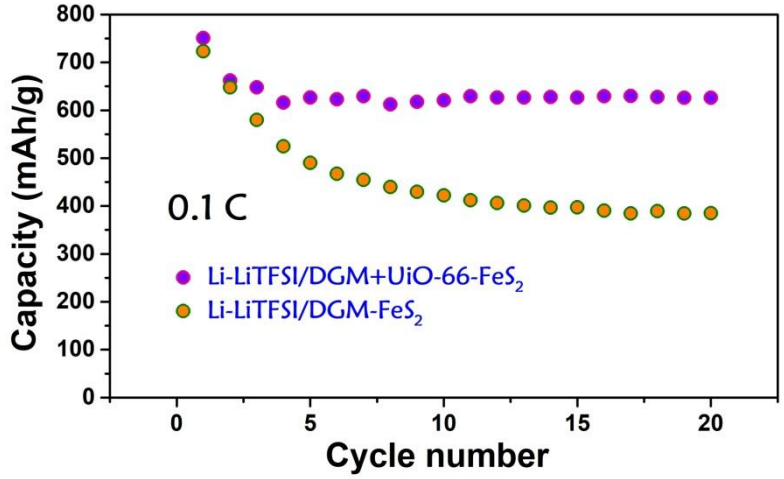

Figure S16. Cycling performance comparison of Li/FeS_2 cells with and without UiO-66 as additive at 0.1C.